

# THE ELECTRICAL PROPERTIES OF LANTHANIDE CO-DOPED CERIA FOR INTERMEDIATE TEMPERATURE SOLID OXIDE ELECTROLYTES

Aliye Arabaci

Istanbul University, Faculty of Engineering, Department of Metallurgical and Materials Engineering, Avcilar, 34320 Istanbul, Turkey  
Corresponding author: Aliye Arabaci, e-mail: [aliye@istanbul.edu.tr](mailto:aliye@istanbul.edu.tr)

REFERENCE NO	ABSTRACT
ELYT-01	Ceria based solid electrolyte materials are very useful for intermediate-temperature solid oxide fuel cell (IT-SOFC) applications. In order to develop intermediate temperature electrolyte materials for solid oxide fuel cells, Gd <sup>3+</sup> and Nd <sup>3+</sup> co-doped ceria based materials Ce <sub>0.80</sub> Gd <sub>0.2-x</sub> Nd <sub>x</sub> O <sub>2-δ</sub> were prepared through the citric-nitrate combustion process. Structures of the samples were studied by X-ray diffraction technique. XRD patterns showed that all samples have fluorite-type crystal structure similar to the undoped ceria. Dense ceramic Ce <sub>0.80</sub> Gd <sub>0.2-x</sub> Nd <sub>x</sub> O <sub>2-δ</sub> electrolyte samples were prepared by sintering the pellets at 1400 °C for 6h. Two probe A.C. impedance spectroscopy was used to study the total ionic conductivity of doped and co-doped ceria ceramics in the temperature range between 300 °C and 800 °C in air atmosphere. The Ce <sub>0.80</sub> Gd <sub>0.12</sub> Nd <sub>0.08</sub> O <sub>1.90</sub> composition demonstrated the maximum ionic conductivity with less activation energy at 800 °C.

*Keywords:*

Ceria, electrolyte, citric-nitrate combustion process.

## 1. INTRODUCTION

Doped-ceria fluorites have been considered as one of the most promising electrolytes for intermediate temperature solid oxide fuel cells (IT-SOFC) due to their high oxygen ion conductivity below 800 °C [1,2]. These materials show much higher ionic conductivity at relatively lower temperatures in comparison to that of the traditional electrolyte yttria-stabilized zirconia (YSZ). Some single element doped electrolytes, such as Ce<sub>1-x</sub>Sm<sub>x</sub>O<sub>2-y</sub> and Ce<sub>1-x</sub>Gd<sub>x</sub>O<sub>2-y</sub> etc., display high oxide ion conductivity. However, some researchers continuously assumed that co-doped ceria should have higher ionic conductivity than single element-doped ceria. Up to now, lowering the operating temperature and reducing the cost of electrolyte materials are the two major problems for the commercialisation of SOFC. With the purpose of further optimizing the properties of the electrolyte material for SOFC applications, co-doping method has been used in recent years. Many studies have been reported that co-doping process may enhance the conductivity even at moderate or intermediate temperatures [3-9].

The ionic conductivity of doped ceria can be influenced by dopant ion type, dopant concentration, oxygen vacancy concentration, defect association energy and local defect structure [10-12]

Inaba and co-worker [10] reported that for single doped ceria in case of rare earth materials, gadolinia doped ceria or samarium doped ceria are the best combinations. For this reason, to prepare co-doped ceria electrolytes with rare earth ions, Gd<sup>3+</sup> and Nd<sup>3+</sup> were selected as co-dopant pairs. In this paper, Gd<sup>3+</sup> and Nd<sup>3+</sup> co-doped ceria based Ce<sub>0.8</sub>Gd<sub>0.2-x</sub>Nd<sub>x</sub>O<sub>1.90</sub> (x = 0.0, 0.04 and 0.08) materials were synthesized through the Pechini Method and characterized. And also, the current paper is intended to study the structure and electrical conductivity of the Nd co-doped ceria in comparison with gadolinium doped ceria (Ce<sub>0.8</sub>Gd<sub>0.2</sub>O<sub>1.90</sub>) and to identify the proper electrolyte composition for SOFC applications.

## 2. EXPERIMENTAL

The samples with the general formula Ce<sub>0.8</sub>Gd<sub>0.2-x</sub>Nd<sub>x</sub>O<sub>1.90</sub> (x = 0.00-0.08) were synthesized using the Pechini Method. High

purity  $\text{Ce}(\text{NO}_3)_3 \cdot 6\text{H}_2\text{O}$ ,  $\text{Gd}(\text{NO}_3)_3 \cdot 6\text{H}_2\text{O}$  and  $\text{Nd}(\text{NO}_3)_3 \cdot 6\text{H}_2\text{O}$  were used as the starting materials. In order to prepare  $\text{Ce}_{0.8}\text{Gd}_{0.2}\text{O}_{1.90}$ ,  $\text{Ce}_{0.8}\text{Gd}_{0.16}\text{Nd}_{0.04}\text{O}_{1.90}$ ,  $\text{Ce}_{0.8}\text{Gd}_{0.12}\text{Nd}_{0.08}\text{O}_{1.90}$  electrolytes, the nitrates were weighed and dissolved in the de-ionized water with the desired concentrations. Citric acid (anhydrous citric acid, Boehringer Ingelheim) was dissolved in de-ionized water and then was added with ethylene glycol (R.P. Normopur) to the cation solution. The molar ratio of total oxide (TO): citric acid (CA) and ethylene glycol: citric acid was selected as 2:1 and 4:1, respectively. The obtained purple solutions were heated and stirred on a hot plate at 80 °C. With the evaporation of water, the solution was gradually transformed into a brown viscous gel. The gel was placed in an oven at 110 °C for 24h. Slowly the gel started to foam, swell and finally burn with glowing flints and the evolution of large amounts of gas occurred. This auto ignition was completed within a few seconds, giving rise to a light green coloured ash, which was calcined at 600 °C for 4h to remove the residual carbonaceous materials and to obtain the most stable mixed metal oxide phase. Oxidation of  $\text{Ce}^{3+}$  to  $\text{Ce}^{4+}$  took place during this stage [2]. The calcined powders were uniaxially pressed at a compaction pressure of 200 MPa into 10 mm diameter pellets and sintering was performed at 1400 °C for 6 h.

The X-ray spectra of Sm and Nd co-doped ceria particles were obtained over the  $2\theta$  range of 10-90° by using Rigaku D/max-2200 ultima X-ray diffractometer with  $\text{CuK}\alpha$  radiation (1.5406 Å). FEI QUANTA FEG 450 scanning electron microscope was used to study the morphology and microstructure of the sintered samples. Impedance measurements were taken by employing SOLARTRON 1260 FRA and 1296 interface at 300, 400 and 800 °C in air atmosphere.

### 3. RESULTS AND DISCUSSIONS

#### 3.1. Phase structure

Fig.1 shows the XRD patterns of  $\text{Ce}_{0.8}\text{Gd}_{0.20}\text{O}_{1.90}$ ,  $\text{Ce}_{0.8}\text{Gd}_{0.16}\text{Nd}_{0.04}\text{O}_{1.90}$ ,

$\text{Ce}_{0.8}\text{Gd}_{0.12}\text{Nd}_{0.08}\text{O}_{1.90}$  powders calcined at 600 °C for 4h. It can be seen that all samples were single phase with cubic fluorite structure (JCPDS powder diffraction file no. 34-0394). There were no other peaks that belong to different phases. The crystallite size ( $D_{\text{XRD}}$ ) is calculated considering the Scherrer equation. The average crystallite size of  $\text{Ce}_{0.80}\text{Gd}_{0.2-x}\text{Nd}_x\text{O}_{1.90}$  sample was in the range of 44-57 nm. The addition of  $\text{Gd}^{3+}$  and  $\text{Nd}^{3+}$  into  $\text{Ce}^{4+}$  may cause a small shift in the Ceria ( $\text{CeO}_2$ ) peaks; this situation indicates a change in the lattice parameter. The lattice parameter (a) of the co-doped ceria can be calculated using the following relation:

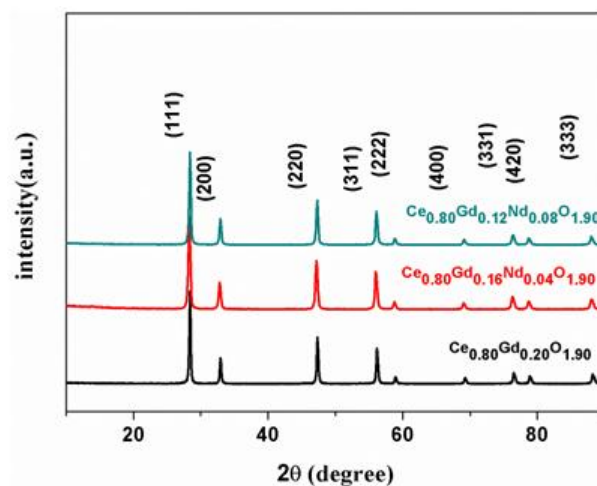


Fig. 1. XRD patterns of the calcined  $\text{Ce}_{0.80}\text{Gd}_{0.20-x}\text{Nd}_x\text{O}_{1.90}$  ( $x = 0-0.08$ ) powders.

$$d = \lambda / 2 \sin\theta, a = d\sqrt{(h^2+k^2+l^2)} \quad (1)$$

where  $d$  is the inter planar spacing,  $\lambda$  is the wavelength of the radiation ( $\text{CuK}\alpha$  ( $\lambda=1.5418$  Å)),  $\theta$  is the diffraction angle, and  $a$  is the lattice parameter.

The lattice parameters of  $\text{Ce}_{0.80}\text{Gd}_{0.20}\text{O}_{1.90}$ ,  $\text{Ce}_{0.80}\text{Gd}_{0.16}\text{Nd}_{0.04}\text{O}_{1.90}$ ,  $\text{Ce}_{0.80}\text{Gd}_{0.12}\text{Nd}_{0.08}\text{O}_{1.90}$  samples were calculated as 5.423, 5.434, 5.439 Å, respectively. The ionic radii of  $\text{Sm}^{3+}$ ,  $\text{Nd}^{3+}$ , and  $\text{Ce}^{4+}$  decrease in the order of  $\text{Nd}^{3+} > \text{Gd}^{3+} > \text{Ce}^{4+}$ ; thus, with more substitution of  $\text{Ce}^{4+}$  with  $\text{Nd}^{3+}$  than  $\text{Gd}^{3+}$ , the volume of the  $\text{CeO}_2$  unit cell will be further enlarged and this may result in a peak shift toward lower  $2\theta$  values.

### 3.2. SEM Images

Fig.2 shows the SEM micrographs of the  $\text{Ce}_{0.80}\text{Gd}_{0.20}\text{O}_{1.90}$ ,  $\text{Ce}_{0.80}\text{Gd}_{0.16}\text{Nd}_{0.04}\text{O}_{1.90}$ ,  $\text{Ce}_{0.80}\text{Gd}_{0.12}\text{Nd}_{0.08}\text{O}_{1.90}$  pellets sintered at 1400 °C for 6h. There are no pores observed on the sample surface, which is consistent with the measured density of the sintered pellet. The calculated relative densities were over 95% of the theoretical densities, which can almost meet the demand for electrolyte materials used in the SOFC applications. The average grain size of the  $\text{Ce}_{0.80}\text{Gd}_{0.20}\text{O}_{1.90}$ ,  $\text{Ce}_{0.80}\text{Gd}_{0.16}\text{Nd}_{0.04}\text{O}_{1.90}$  samples were found to be in the range of 0.25-0.96  $\mu\text{m}$ . The average grain size of  $\text{Ce}_{0.80}\text{Gd}_{0.12}\text{Nd}_{0.08}\text{O}_{1.90}$  found to be in the range of 0.2-1.25  $\mu\text{m}$ . The  $\text{Ce}_{0.80}\text{Gd}_{0.12}\text{Nd}_{0.08}\text{O}_{1.90}$  pellet showed larger grains corresponding to a smaller grain boundary volume, which might be the reason for higher total conductivity observed for 8 mol % Nd doped ceria sample.

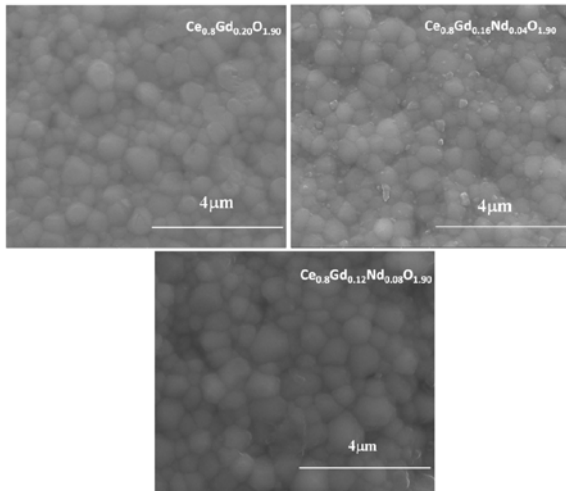


Fig. 2. SEM image of the surface of the sintered  $\text{Ce}_{0.8}\text{Gd}_{0.2-x}\text{Nd}_x\text{O}_{1.90}$  ( $x = 0.0-0.08$ ) pellet.

### 3.3. Electrical Conductivity

In case of doped ceria electrolyte materials, the main contribution of the conductivity in air is ionic conductivity [10] and the contribution of electronic conductivity is negligible [13].

The conductivity ( $\sigma$ ) was calculated from resistance, thickness L, cross-sectional area A, using Eq. (2)

$$\sigma = L / RA \quad (2)$$

The activation energy for conduction is obtained by plotting the ionic conductivity data in the Arrhenius relation for thermally activated conduction. The Activation energy for the conduction calculated using Eq. (3),

$$\sigma = \frac{\sigma_0}{T} \exp \frac{E = \Delta H_m \pm \Delta H_a}{kT}$$

where T is the temperature in K,  $\sigma$  is the total conductivity at temperature T,  $\sigma_0$  is a pre-exponential factor, E is the activation energy, and k is the Boltzmann's constant.  $\Delta H_m$  and  $\Delta H_a$  denote the migration enthalpy and association enthalpy of the oxygen vacancy, respectively.  $\sigma_0$  is related to the oxygen vacancy concentration and vibrational frequency of the lattice.

Fig.3 displays an impedance spectrum for  $\text{Ce}_{0.80}\text{Gd}_{0.12}\text{Nd}_{0.08}\text{O}_{1.90}$  at different temperatures in the frequency range (100 mHz – 10 MHz). For each composition impedance data was recorded and  $\text{Ce}_{0.80}\text{Gd}_{0.12}\text{Nd}_{0.08}\text{O}_{1.90}$  composition can be observed in Fig 3. Impedance spectrum of the samples at 300 °C and 400 °C consists in a semicircle with decreasing grain resistance ( $R_g$ ), grain boundary resistance ( $R_{gb}$ ) and electrode effect ( $R_e$ ).

Complex impedance spectra plots of the  $\text{Ce}_{0.80}\text{Gd}_{0.2-x}\text{Nd}_x\text{O}_{1.90}$  ( $x=0.00, 0.04$  and  $0.08$ ) pellets sintered at 1400 °C were measured at 800 °C and can be seen in Fig.4. At 800 °C, Fig.4 shows that the spectrum consists of one semicircle. At this temperature, the grain ( $R_g$ ) and grain boundary ( $R_{gb}$ ) resistances are not discrete; only the total conductivity can be calculated. At 800 °C, the conductivity of  $\text{Ce}_{0.80}\text{Gd}_{0.12}\text{Nd}_{0.08}\text{O}_{1.90}$  ( $E_a = 0.67$  eV) was 8.3 % higher than the conductivity of  $\text{Ce}_{0.80}\text{Gd}_{0.20}\text{O}_{1.90}$  ( $E_a = 0.70$  eV).

Lenka et al. [14] reported that the grain conductivity increases with an increase in grain size, and grain boundary conductivity decreases with an increase in grain size. Same trend was also observed in this study. From SEM results, it was recognized that the  $\text{Ce}_{0.80}\text{Gd}_{0.12}\text{Nd}_{0.08}\text{O}_{1.90}$  pellet had larger grains than other samples corresponding to a smaller grain boundary volume.

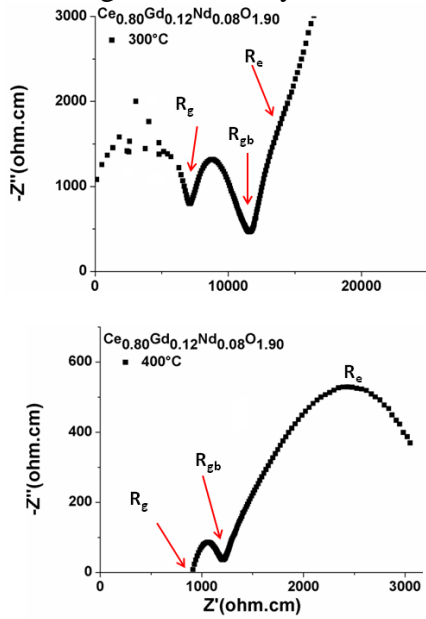


Fig.3. Complex impedance spectra plots of the  $\text{Ce}_{0.80}\text{Gd}_{0.2-x}\text{Nd}_{0.08}\text{O}_{1.90}$  ( $x=0.08$ ) pellet sintered at  $1400\text{ }^{\circ}\text{C}$ , and measured at  $300\text{ }^{\circ}\text{C}$  and  $400\text{ }^{\circ}\text{C}$  in air. The grain, grain boundary and electrode contributions are represented as  $R_g$ ,  $R_{gb}$  and  $R_e$ , respectively.

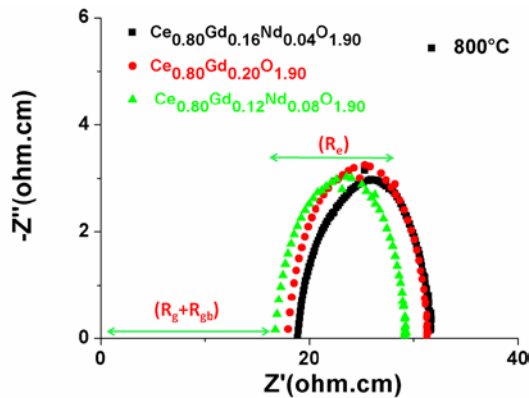
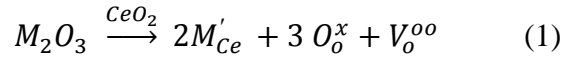


Fig.4. Complex impedance spectra plots of the  $\text{Ce}_{0.80}\text{Gd}_{0.2-x}\text{Nd}_{0.08}\text{O}_{1.90}$  ( $x=0.00, 0.04$  and  $0.08$ ) pellets sintered at  $1400\text{ }^{\circ}\text{C}$ , measured at  $800\text{ }^{\circ}\text{C}$  in air.

In ceria ( $\text{CeO}_2$ ) lattice, oxide vacancies ( $V_o^{oo}$ ) may be introduced by ceria reduction or by doping with oxides of metals with lower valences (such as;  $\text{Gd}^{3+}$ ,  $\text{Sm}^{3+}$ ,  $\text{Ca}^{2+}$  etc). These

equations are written in Kroger-Vink notation [10, 11].



Pure ceria materials are mixed ionic–electronic conductors with a limited concentration of oxygen vacancies. However, when doped with rare earth elements, additional oxygen vacancies may be generated for the compensation of charge difference between dopants with +3 charges (M: Gd, Nd) and host cations with +4 charges, which may increase the overall ionic conductivity. Namely, the ionic conductivities are significantly enhanced in  $\text{Ce}_{0.80}\text{Gd}_{0.2-x}\text{Nd}_x\text{O}_{1.90}$  ceramics by increasing oxygen vacancies. Further, the oxide ion mobility increases with increasing temperature, so the conductivity increases at high temperatures. Thus, at  $800\text{ }^{\circ}\text{C}$ , the  $\text{Ce}_{0.80}\text{Gd}_{0.12}\text{Nd}_{0.08}\text{O}_{1.90}$  electrolyte material demonstrated better total ionic conductivity than the single doped ceria ( $\text{Ce}_{0.80}\text{Gd}_{0.20}\text{O}_{1.90}$ ).

### 3. CONCLUSIONS

Gadolinium and Neodymium co-doped ceria samples  $\text{Ce}_{0.80}\text{Gd}_{0.2-x}\text{Nd}_x\text{O}_{1.90}$  ( $x=0, 0.04, 0.08$ ) were successfully prepared through the Pechini Method. Gadolinium and Neodymium co-doped ceria powders calcined at  $600\text{ }^{\circ}\text{C}$  showed only a cubic fluorite structure like pure ceria. The pellets were sintered at  $1400\text{ }^{\circ}\text{C}$  for 6h to obtain dense ceramics and the calculated relative densities were over 95% of the theoretical densities. Lattice parameter increased linearly with the increasing dopant concentration.

According to the electrochemical impedance spectroscopy results,  $\text{Ce}_{0.80}\text{Gd}_{0.20}\text{O}_{1.90}$  exhibited a total conductivity of  $5.55 \times 10^{-2}\text{ S cm}^{-1}$ ,  $\text{Ce}_{0.80}\text{Gd}_{0.16}\text{Nd}_{0.04}\text{O}_{1.90}$  showed a total conductivity of  $5.25 \times 10^{-2}\text{ S cm}^{-1}$  and  $\text{Ce}_{0.80}\text{Gd}_{0.12}\text{Nd}_{0.08}\text{O}_{1.90}$  displayed a total conductivity of  $6.01 \times 10^{-2}\text{ S cm}^{-1}$  at  $800\text{ }^{\circ}\text{C}$ . The composition  $\text{Ce}_{0.80}\text{Gd}_{0.12}\text{Nd}_{0.08}\text{O}_{1.90}$  showed the highest total ionic conductivity and minimum activation energy ( $E_a=0.67\text{ eV}$ ) in the current series. Thus,

$Ce_{0.80}Gd_{0.12}Nd_{0.08}O_{1.90}$  can be defined as a more promising electrolyte material for IT-SOFC based applications considering the results of the present study.

### Acknowledgements

The authors gratefully acknowledge the Financial Support of the Scientific Research Projects Coordination Unit of İstanbul University.

### References

- [1] Hideaki I., Ceria-based solid electrolytes, *Solid State Ionics*, Vol 83, 1996, pp. 1–16.
- [2] Steele, B.C.H., Appraisal of  $Ce_{1-y}Gd_yO_{2-y/2}$  electrolytes for IT-SOFC operation at 500°C, *Solid State Ionics*, Vol 129, 2000, pp. 95–110.
- [3] T. Mori, J. Drennan, J.H. Lee, J.G. Li, T. Ikegami, Oxide ionic conductivity and microstructures of Sm- or La-doped  $CeO_2$ -based systems, *Solid State Ionics*, Vol.154-155, 2002, pp. 461-466.
- [4] H. Yoshida, T. Inagaki, K. Miura, M. Inaba, Z. Ogumi, Density functional theory calculation on the effect of local structure of doped ceria on ionic conductivity, *Solid State Ionics*, Vol.160, No. 1-2, 2003, pp.109-116.
- [5] V. P. Kumar, Y. S. Reddy, P. Kistaiah, G. Prasad and C. V. Reddy, Thermal and electrical properties of rare-earth co-doped ceria ceramics, *Mater. Chem. Phys.*, Vol.112, No.2, 2008, pp. 711-718.
- [6] S. Ramesh and C. V. Reddy, Electrical Properties of Co-Doped Ceria Electrolyte  $Ce_{0.8-x}Gd_{0.2}Sr_xO_{2-\delta}$  ( $0.0 \leq x \leq 0.1$ ), *Acta Phys. Polon. A*, Vol. 115, No.5, 2009, pp.909-913.
- [7] S. Ramesh, V. P. Kumar, P. Kistaiah and C. V. Reddy, Preparation, characterization and thermo electrical properties of co-doped  $Ce_{0.8-x}Sm_{0.2}Ca_xO_{2-\delta}$  materials, *Solid State Ionics*, Vol. 181, No.1-2, 2010, pp. 86-91.
- [8] F. Y. Wang, B. Z. Wan and S. Cheng, Study on  $Gd^{3+}$  and  $Sm^{3+}$  co-doped ceria-based electrolytes, *J. Solid State Electrochem.*, Vol. 9, No.3, 2005, pp.168-173.
- [9] F. Y. Wang, S. Chen, Q. Wang, S. Yu and S. Cheng, Study on Gd and Mg co-doped ceria electrolyte for intermediate temperature

solid oxide fuel cells, *Catal.Today*, Vol. 97, No.2-3,2004, pp.189-194.

- [10] H. Inaba and H. Tagawa, Ceria-Based Solid Electrolytes, *Solid State Ionics*, 83 [1–2] 1–16 (1996)
- [11] J. A. Kilner, Fast oxygen transport in acceptor doped oxides, *Solid State Ionics*, Vol.129, No.1-4, 2000, pp.13-23.
- [12] H. Yoshida, T. Inagaki, K. Miura, M. Inaba and Z. Ogumi, Density functional theory calculation on the effect of local structure of doped ceria on ionic conductivity, *Solid State Ionics*, Vol.160, No.1-2, 2003, pp. 109-116.
- [13] G. M. Christie and F. P. F. Van Berkel, Microstructure - Ionic Conductivity Relationships in Ceria-Gadolinia Electrolytes, *Solid State Ionics*, Vol.83, No.1–2, 1996, pp.17–27.
- [14] R.K. Lenka, T. Mahata, A.K. Tyagi, P.K. Sinha, Influence of grain size on the bulk and grain boundary ion conduction behavior in gadolinia-doped ceria, *Solid State Ionics*, Vol.181, 2010, pp.262–267.